



# Refractory dissolved organic matters in sludge leachate trigger the combination of anammox and denitrification for advanced nitrogen removal

Ben Dai<sup>a,c</sup>, Yifeng Yang<sup>b,\*</sup>, Zuobin Wang<sup>a,d</sup>, Jingzhou Zhou<sup>a,c</sup>, Zhenyu Wang<sup>a,c</sup>, Xin Zhang<sup>b</sup>, Siqing Xia<sup>a,c,\*</sup>

<sup>a</sup> State Key Laboratory of Pollution Control and Resource Reuse, College of Environmental Science and Engineering, Tongji University, Shanghai 200092, China

<sup>b</sup> Shanghai Municipal Engineering Design Institute (Group) Co., Ltd, Shanghai 200092, China

<sup>c</sup> Shanghai Institute of Pollution Control and Ecological Security, Shanghai 200092, China

<sup>d</sup> National Engineering Research Center of Dredging Technology and Equipment, Shanghai, China

## ARTICLE INFO

### Keywords:

Sludge leachate  
Refractory dissolved organic matter (rDOM)  
Anammox  
Denitrification  
Advanced nitrogen removal  
Spectroscopic analysis of rDOM

## ABSTRACT

The cost-effective treatment of sludge leachate (SL) with high nitrogen content and refractory dissolved organic matter (rDOM) has drawn increasing attention. This study employed, for the first time, a rDOM triggered denitrification-anammox continuous-flow process to treat landfill SL. Moreover, the mechanisms of exploiting rDOM from SL as an inner carbon source for denitrification were systematically analyzed. The results demonstrated outstanding nitrogen and rDOM removal performance without any external carbon source supplement. In this study, effluent concentrations of  $4.27 \pm 0.45$  mgTIN/L and  $5.58 \pm 1.64$  mgTN/L were achieved, coupled with an impressive COD removal rate of  $65.17\% \pm 1.71\%$ . The abundance of bacteria belonging to the *Anaerolineaceae* genus, which were identified as rDOM degradation bacteria, increased from 18.23% to 35.62%. As a result, various types of rDOM were utilized to different extents, with proteins being the most notable, except for lignins. Metagenomic analysis revealed a preference for directing electrons towards  $\text{NO}_3^-$ -N reductase rather than  $\text{NO}_2^-$ -N reductase, indicating the coupling of denitrification bacteria and anammox bacteria (*Candidatus Brocadia*). Overall, this study introduced a novel synergy platform for advanced nitrogen removal in treating SL using its inner carbon source. This approach is characterized by low energy consumption and operational costs, coupled with commendable efficiency.

## 1. Introduction

It is estimated that globally, over 300 million tons of waste sludge are produced annually from sewage treatment plants (Song et al., 2024). Over the years, landfilling has been the conventional method for municipal sludge treatment due to its simplicity and cost advantage in handling large quantities of sludge (Xu et al., 2021). However, such a disposal process has led to a new issue of the production of sludge leachate (SL) in aged landfill, posing adverse risks to the ecological environment and human health (Renou et al., 2008; Zhang et al., 2022a). The SL in aged landfills exhibited a high enrichment of ammonia ( $> 500$  mg/L) and refractory dissolved organic matters

(rDOM), originating from the hydrolysis of extracellular polymeric substances and biomass decay (Wu et al., 2023). Notably, the content of rDOM in SL such as humic substances, lignin, recalcitrant dissolved organic nitrogen (ON) etc. usually is close to the COD value in mature leachate owing to the extremely low concentration of biodegradable organic compounds (Chen et al., 2024; He et al., 2015; Wang et al., 2019). However, employing conventional biological nitrogen removal methods for treating aged landfill SL is challenging due to its low COD/TN ratio (less than 1.5) and low BOD/COD (less than 0.2).

Notably, compared to conventional nitrogen removal process, the anammox method has been recognized as the most cost-effective and environmentally friendly approach for nitrogen removal, well-suited for

**Abbreviations:** Anammox, anaerobic ammonium oxidation; SL, sludge leachate; rDOM, refractory dissolved organic matter; TIN, total inorganic nitrogen; TN, total nitrogen; ON, organic nitrogen; C/N, COD/TN; HRT, hydraulic retention time; UASB, up flow anaerobic sludge blanket; RS,  $\text{NO}_2^-$ -N/ $\text{NH}_4^+$ -N ratio; EEM, excitation emission matrix; FI, fluorescence index; HIX, humification index; BIX, biological index;  $\Delta$ RP,  $\Delta\text{NO}_3^-$ -N/ $\Delta\text{NH}_4^+$ -N;  $\Delta$ RS,  $\Delta\text{NO}_2^-$ -N/ $\Delta\text{NH}_4^+$ -N; SMP, soluble microbial product; PARAFAC analysis, parallel factor analysis; FTICR-MS, Fourier transform ion cyclotron resonance-mass spectrometry analysis.

\* Corresponding authors.

E-mail addresses: [yangyifeng@smedi.com](mailto:yangyifeng@smedi.com) (Y. Yang), [siqingxia@tongji.edu.cn](mailto:siqingxia@tongji.edu.cn) (S. Xia).

<https://doi.org/10.1016/j.watres.2024.121678>

Received 23 February 2024; Received in revised form 19 April 2024; Accepted 24 April 2024

Available online 25 April 2024

0043-1354/© 2024 Elsevier Ltd. All rights reserved.

**Table 1**  
Operational conditions of anammox-UASB in different phases.

Stage	Time (d)	TN <sup>a</sup> (inf.) (mg/L)	TIN <sup>b</sup> (inf.) (mg/L)	NH <sub>4</sub> <sup>+</sup> -N (inf.) (mg/L)	NO <sub>2</sub> <sup>-</sup> -N/ NH <sub>4</sub> <sup>+</sup> -N (inf., avg.)	COD/TIN (inf., avg.)	Ratio of SL (%) <sup>c</sup>
I	1–53	464–1214	464–1214	200–523	1.32	0	0
II-1	54–67	975–1083	950–1050	442–456	1.21	0.13	20
II-2	68–81	887–906	830–836	429–434	1.15	0.31	40
II-3	82–95	1040–1064	924–936	429–434	0.93	0.56	80
III	96–200	945–1190	800–1037	443–530	0.88	0.72	100

Note:

<sup>a</sup> TN represents total nitrogen.

<sup>b</sup> TIN represents total inorganic nitrogen, including NH<sub>4</sub><sup>+</sup>-N, NO<sub>2</sub><sup>-</sup>-N and NO<sub>3</sub><sup>-</sup>-N.

<sup>c</sup> Ratio of SL to influent was calculated based on the NH<sub>4</sub><sup>+</sup>-N.

the treatment of wastewater with low C/N ratio (Dai et al., 2023). However, relying solely on anammox process makes it challenging to achieve deep nitrogen removal, leaving approximately 11 % of nitrogen presented in nitrate unrecovered (Kartal et al., 2010). Denitrification (nitrate to nitrite) is a biological process capable of nitrate reduction, with the produced nitrite serving as an extra substrate supply for anammox (Du et al., 2019). Hence, coupling denitrification with anammox process holds the potential for achieving advanced nitrogen removal in treating SL.

Current studies mainly improved the nitrogen removal performance of leachate by adding extra carbon sources to reduce by-product nitrate, while neglected the function of the *in-situ* rDOM. Therefore, in previous studies, extra carbon source was usually dosed to anammox reactor in order to trigger full or partial denitrification for by-product nitrate reduction and enhancing nitrogen removal process (Du et al., 2015; Hou et al., 2024; Wu et al., 2018; Zhang et al., 2022a; Zhang et al., 2021; Zhang et al., 2022b). However, an excess of carbon sources could lead to the collapse of anammox system, which also increased the costs (Xiao et al., 2021; Zhang et al., 2022b).

Though a partial nitrification process usually be added prior to anammox, only the biodegradable DOM could be removed, the removal of rDOM such as polycyclic aromatic and polyphenols compounds is negligible (Chen et al., 2020; de Graaff et al., 2011; Li et al., 2018). Even more, there is few biodegradable DOM in aged landfill SL. Therefore, there is still a significant amount of rDOM in the supernatant liquor that should be considered after partial nitrification treatment.

Considering the significant degradation of rDOM in landfill leachate during the anammox process (Cao et al., 2019; Jiang et al., 2023; Li et al., 2018; Wang et al., 2019; Xiong et al., 2023), it is presumed that the presence of rDOM in SL could provide possibility for triggering the denitrification process through supplying inadequate electron donor which can provide nitrite for anammox and achieve *in-situ* reduction of nitrate produced by anammox. Although some studies have demonstrated that *in-situ* rDOM in wastewater, enhances nitrogen removal through extending hydraulic retention time, prolonging sludge retention time and bioaugmentation (Cao et al., 2019; Liu et al., 2024; Wu et al., 2022; Xie et al., 2023), these studies primarily focused on the feasibility and enhancement of rDOM utilization. Whether rDOM could trigger denitrification-anammox process and its transformation mechanisms within such a nitrogen removal pathway remains unexplored.

To sum up, the integration of denitrification and anammox presents a promising nitrogen removal process for treating SL. Denitrification utilizes by-product nitrate to supply nitrite for anammox. Simultaneously, rDOM in SL acts as an electron donor, eliminating the requirement for additional carbon sources. Therefore, the aim of this study was to develop a rDOM triggered synergy platform for SL treatment and explore its performance and mechanisms. The primary objectives were: (1) Achieving advanced nitrogen removal including inorganic and organic nitrogen from actual SL using denitrification-anammox process. (2) Utilizing rDOM to achieve denitrification and applying spectroscopic techniques to reveal the transformation mechanisms of rDOM. (3) Unveiling the synergistic mechanisms of denitrification and anammox through

metagenome analysis.

## 2. Materials and methods

### 2.1. Reactor set-up and operations

A lab-scale up flow anaerobic sludge blanket (UASB) reactor with an effective volume of 1.5 L was established for anammox process (Fig. S1). Throughout the experiment, the temperature was maintained at 35 ± 1 °C, and the reflux ratio was set at 12. The hydraulic retention time (HRT) was controlled at 8 h. The pH value of influent was maintained at 7.0–7.5 using 1 M HCl and 1 M NaOH.

The seeding granular anammox sludge was derived from our lab-scale anammox membrane bio-reactor (MBR) that maintained a stable nitrogen removal efficiency exceeding 85 %. The MLSS and MLVSS after inoculation were 19.36 and 15.79 g/L, respectively. No sludge discharge was carried out during the whole experiment. SL with a low-level biodegradable organic matter was collected from the sludge landfill pit inside a large sewage treatment plant in Shanghai and stored at 4 °C. The sampling interval for the triplicate samples was 24 h. The main characteristics of SL were listed in Table S1.

The operation was divided into three stages, as summarized in Table 1. Stage I (1–53 d) is the start-up and stabilization period of the reactor, where the NH<sub>4</sub><sup>+</sup>-N load was gradually increased to 523 mg/L. In this stage, the UASB reactor was continuously fed with synthetic wastewater contained NH<sub>4</sub><sup>+</sup>-N, and NO<sub>2</sub><sup>-</sup>-N (NO<sub>2</sub><sup>-</sup>-N / NH<sub>4</sub><sup>+</sup>-N ratio (RS) = 1.32). Meanwhile, trace elements and minerals were added to the synthetic wastewater to meet the nutritional requirements of microorganisms (Text. S1) (Zhou et al., 2022).

During the subsequent operations, the influent NH<sub>4</sub><sup>+</sup>-N was controlled at 450 ± 50 mg/L, equivalent to its concentration in SL. In Stage II, the NH<sub>4</sub><sup>+</sup>-N ratio supplied by actual sludge leachate (SL) was raised gradually (0 %, 20 %, 40 %, 80 %) when the reactor's effluent remained stable (effluent N species had ≤ 5 % variation for at least 3 days) (Zhou et al., 2022). In Stage III, the SL was stably treated in the UASB reactor where NH<sub>4</sub><sup>+</sup>-N comes entirely from SL. During the SL treatment in anammox reactor (Stage II and III), NO<sub>2</sub><sup>-</sup>-N was provided by the synthetic wastewater.

### 2.2. Spectroscopic measurements of rDOM

#### 2.2.1. Ultraviolet/Visible analysis

The rDOM concentration in the influent and effluent of the reactor was measured via Ultraviolet/Visible (UV-vis) analysis by using a Shimadzu UV-2700. In this analysis, the wavelengths ranged from 220 to 400 nm with a scanning interval of 1 nm. All samples were used for UV-vis analysis without dilution.

#### 2.2.2. EEM fluorescence spectroscopy and PARAFAC analysis

All inlet and outlet samples used for excitation emission matrix (EEM) fluorescence analysis were diluted 100 times to achieve UV<sub>254</sub> below 0.05 cm<sup>-1</sup> (Lu et al., 2017). Fluorescence EEM spectroscopy

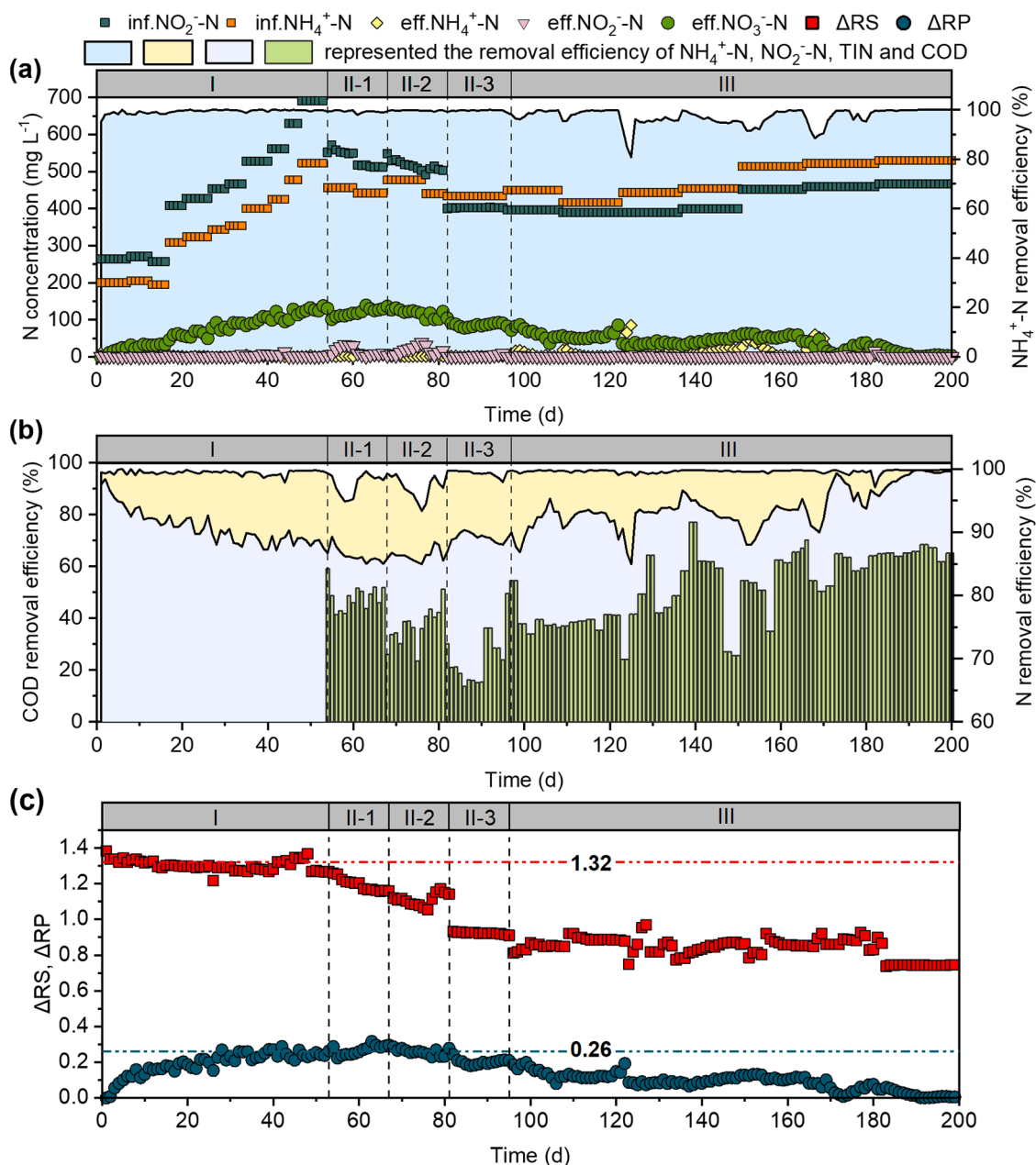


Fig. 1. Long-term performance of anammox-UASB in 200 days. (a) nitrogen removal performance, (b) NO<sub>2</sub><sup>-</sup>-N, TIN and COD removal performance, (c) the ratios of  $\Delta\text{NO}_2^- \text{-N} / \Delta\text{NH}_4^+ \text{-N}$  ( $\Delta\text{RS}$ ) and  $\Delta\text{NO}_3^- \text{-N} / \Delta\text{NH}_4^+ \text{-N}$  ( $\Delta\text{RP}$ ).

measurements results were obtained from a Hitachi F-7000 fluorescence spectrophotometer (Hitachi, Japan). The excitation and emission wavelengths ranged from 200 to 550 nm at intervals of 5 nm and at a scan rate of 12,000 nm/min, respectively. The parallel factor (PARAFAC) modelling analysis was performed in MATLAB 9.0 with the DOMFluor toolbox (Jia et al., 2017). EEM fluorescence data were modelled according to the recommended procedures. The number of fluorescence components was determined by residual analysis, visual inspection and split half analysis. Quantitative comparisons of fluorescence components spectra were applied based on the OpenFluor spectral database (Jia et al., 2017; Osburn et al., 2016). In addition, fluorescence parameters including fluorescence index (FI), humification index (HIX) and biological index (BIX) were analyzed (Text. S2).

### 2.2.3. Fourier transform ion cyclotron resonance-mass spectrometry analysis (FTICR-MS)

The influent and effluent during the stable period of Stage III were collected and filtered through a 0.45- $\mu\text{m}$  filter. The filtered samples were acidified with formic acid to pH = 2, and then extracted by solid phase extraction (Agilent Bond Elut PPL, 1.0 g, 6 mL). The calibration involved a 10 mmol/L sodium formate for the instrument, and all detected quality errors were under 1 ppm. Then, FTICR-MS spectra were acquired using a 15 T Bruker Solarix mass spectrometer (Bruker Daltonics, Bremen, Germany). The detailed extraction steps and specific test parameters were shown in Text. S3. Utilizing the van Krevelen (VK) diagram to visually represent elemental proportions. According to the measured O:C and H:C ratios, rDOM molecules can be divided into seven classes (Text. S4).

### 2.3. Sequencing and bioinformatics analyses

Samples of sludge at the end of each stage (Stage I, Stage II-1, Stage II-2, Stage II-3 and Stage III) were taken for sequencing and bioinformatics analyses. The microbial community was characterized using 16S rRNA sequencing analysis with the primer pair 338F–806R targeting the V3-V4 region. Sequencing of amplicons was conducted on the Illumina Miseq platform (Majorbio, China) according to a previous study (Zhou et al., 2022). In addition, we further analyzed carbon and nitrogen metabolism through metagenomic sequencing analysis using the Illumina HiSeq 2500 platform (Majorbio, China) (Wang et al., 2022a). The obtained metagenomic data were annotated and classified in terms of species and functions based on NR, COG and KEGG databases. All data from DNA samples' sequencing were deposited at the National Center for Biotechnology Information (NCBI)/Sequence Read Archive (SRA) under project PRJNA1067285.

### 2.4. Other analytical methods

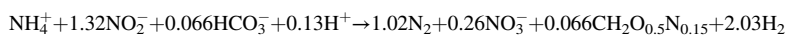
Effluent samples were collected daily and filtered through a 0.45- $\mu\text{m}$  filter immediately for chemical analysis. The parameters including  $\text{NH}_4^+\text{-N}$ ,  $\text{NO}_2^-\text{-N}$ ,  $\text{NO}_3^-\text{-N}$ , MLVSS and MVSS were analyzed in accordance with standard methods (Apha, 1985). Total nitrogen (TN, including inorganic and organic nitrogen) was measured by Shimadzu TOC-L, where organic nitrogen is equal to TN minus total inorganic nitrogen (TIN). COD was analyzed using the spectrophotometer (HACH Model DR 3900). The morphology and structure of granular and floc sludge were observed with a scanning electron microscope (SEM) device (Gemini SEM 300, Germany).

## 3. Results and discussion

### 3.1. Performance of anammox-UASB treating sludge leachate

#### 3.1.1. Inorganic nitrogen removal performance

The anammox-UASB was operated for 200 days with three stages based on the  $\text{NH}_4^+\text{-N}$  ratio supplied by actual SL. In Stage I (day 1–53), synthetic wastewater with continuously increasing nitrogen load (TIN from 464 to 1214 mg/L) was fed to the reactor to obtain a stable anammox system for SL treatment. In Stage I, the effluent  $\text{NH}_4^+\text{-N}$  and  $\text{NO}_2^-\text{-N}$  were  $1.86 \pm 1.75$  mg/L and  $2.43 \pm 1.96$  mg/L, respectively. Simultaneously, the concentration of  $\text{NO}_3^-\text{-N}$  was constantly increasing (Fig. 1a). As a result, the TIN removal efficiency was decreasing and the calculated effluent nitrite production rate ( $\Delta\text{NO}_3^-\text{-N} / \Delta\text{NH}_4^+\text{-N}$ ,  $\Delta\text{RP}$ ) was increasing in the initial 15 days, and finally stabilized at  $89.05 \pm 1.20 \%$  and  $0.25 \pm 0.02$ , respectively (Fig. 1b, c). Also, the  $\Delta\text{NO}_2^-\text{-N} / \Delta\text{NH}_4^+\text{-N}$  ( $\Delta\text{RS}$ ) maintained at  $1.30 \pm 0.03$  (Fig. 1c), which approached the theoretical stoichiometric value of the anammox process (Du et al., 2023). This phenomenon indicated the fantastic anammox performance in Stage I was achieved.



In Stage II (day 54–95), actual SL was fed into the reactor gradually (from 20 % to 80 %).  $99.53 \pm 0.37 \%$  of  $\text{NH}_4^+\text{-N}$  removal efficiency was achieved. However, nitrite accumulated in Stage II-1 (Fig. 1a). Therefore, we speculate that the denitrification process was highly likely triggered by the input of SL in this anammox reactor (Du et al., 2019). We decreased the influent RS to 1.21 in Stage II-1.  $87.22 \pm 1.62 \%$  of TIN removal efficiency were achieved (Fig. 1a, b). Interestingly, nitrite

accumulated again in Stage II-2 (Fig. 1a). Hence, with the heightened proportion of SL in the influent, the denitrification which utilized the nitrate produced from anammox process was also enhanced. In order to improve nitrogen removal efficiency, we further decreased the influent RS to 1.15 in Stage II-2 and 0.93 in Stage II-3. A better nitrogen removal performance with  $89.06 \pm 0.85 \%$  of TIN removal efficiency was achieved. However, with the increasing of SL ratio, the COD removal efficiency decreased firstly and then increased in Stage II. This could be attributed to that some microorganisms could utilize rDOM in the SL gradually enriched (Cao et al., 2019; Du et al., 2022). These phenomena also indicate the potential for rDOM in SL to trigger denitrification.

In Stage III, 100 % of SL was fed into the reactor. We further reduced the influent RS to 0.88 to prevent the accumulation of nitrite due to the increasing SL ratio. The extremely low influent RS also posed a challenge to the anammox system (Jiang et al., 2022). Excitingly,  $\text{NH}_4^+\text{-N}$  removal efficiency maintained at  $98.36 \pm 1.82 \%$  and  $\text{NO}_3^-\text{-N}$  in effluent gradually decreased to 3.02 mg/L. Also, the COD removal efficiency gradually increased (stabled at  $65.17 \pm 1.71 \%$ ), which proved that the low influent RS resulted in more demand for nitrite generated via denitrification and enhanced the utilization of rDOM. Significantly, the TIN removal efficiency increased and stabled at  $99.58 \pm 1.34 \%$ . Meanwhile, the effluent TIN was also less than 5 mg/L in the stable period of Stage III. Slightly  $\text{NO}_3^-\text{-N}$  in effluent indicated the available rDOM was sufficiently utilized. Hence, a hybrid autotrophic–heterotrophic process was developed, with advanced nitrogen removal of SL utilizing the *in-situ* rDOM.

#### 3.1.2. Organic nitrogen removal performance

In the UASB reactor, the organic nitrogen (ON) removal also achieved a fantastic performance. As shown in Fig. 2, the ON removal efficiency gradually increased in the long-term SL treatment process, which has a similar tendency to the removal of COD (Fig. 1b). Excitingly, in the later of Stage III, the effluent ON maintained at  $1.76 \pm 1.38$  mg/L, with a removal efficiency of  $99.05 \pm 0.87 \%$ . These results indicated that the anammox-UASB has achieved perfect nitrogen removal performance ( $5.58 \pm 1.64$  mgTN/L), encompassing both organic and inorganic nitrogen (Figs. 1 and 2). The fantastic removal efficiency of ON could be attributed to the involvement of denitrification process (Yin et al., 2023). Therefore, these findings also suggested an enhanced denitrification process using recalcitrant dissolved organic nitrogen (rDON) (Zhang et al., 2020).

### 3. 2 rDOM in sludge leachate functioned as the electron donor of nitrate reduction

#### 3.2.1. Ultraviolet/Visible analysis unveiled the degradation of rDOM

The excellent nitrogen removal performance was associated with a stable electron donor source in the anammox system (Jiang et al., 2023). Therefore, as the most potential electron donors in SL, rDOM was subjected to a series of spectroscopic measurements to evaluate its role in

nitrate removal.

The UV–vis absorption spectra of influent and effluent were obtained (Fig. 3a). The strong DOM absorption was evident between 260 nm and 400 nm, indicating that the dominant components of rDOM in SL were mainly short-wavelength-absorbing chromophores and auxochromes (Li et al., 2018). As shown in Fig. 3a, the effluent absorbance generally exhibited lower intensity compared to the influent that suggesting a reduction in some organic matter content (Chen et al., 2019). Both

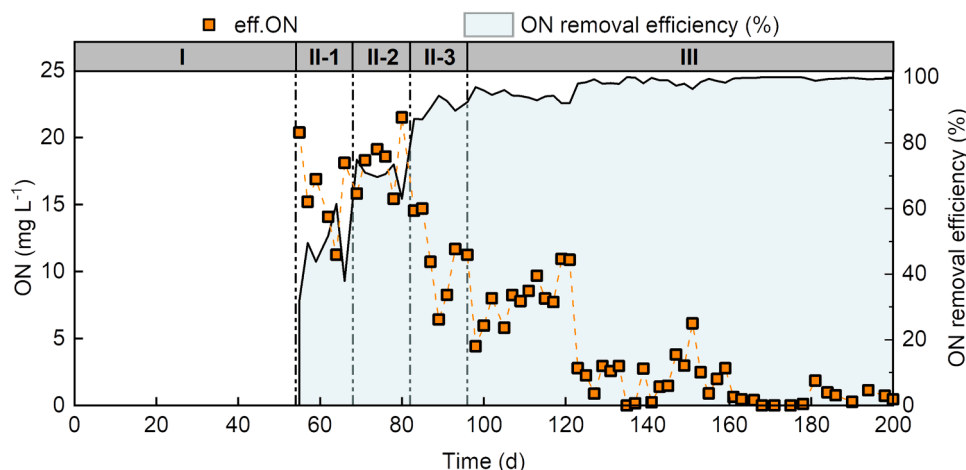


Fig. 2. Long-term removal performance of organic nitrogen (ON) in anammox-UASB reactor.

UV254 and UV280 decreased post-anammox treatment, especially in wavelength 340–380 nm the absorbance decreased dramatically, suggesting a reduction in aromatic compounds containing C=C, C=O, and hydrophobic properties (Li et al., 2018). The UV250/UV365 ratio exhibited a negative correlation with the humus molecular weight, which increased from  $2.31 \pm 0.39$  to  $7.19 \pm 0.94$  during the anammox process, indicating a decline in the molecular weight of humus in the leachate (Chen et al., 2019; Jiang et al., 2023). These observations indicated that a series of aromatic compounds and humus in rDOM were degraded, coupling with the nitrogen removal process.

### 3.2.2. Fluorescence EEM-PARAFAC analysis indicated the utilization of rDOM

The influent and effluent samples in Stage II & III were collected for EEM fluorescence spectroscopy analyze to investigate the utilization of rDOM in this system (Fig. 3b-c). Two peaks (peak A and B) were identified in influent samples, while three peaks (peak A, B and C) were identified in effluent samples. Therefore, peak C (Ex/Em = 230 nm/350 nm) might be a fresh soluble microbial product (SMP) or the fluorescence peak of degradation product (Jiang et al., 2023). In addition, peak A (Ex/Em = 250 nm/450 nm) and B (Ex/Em = 280 nm/350 nm) decreased remarkably after treatment, suggesting that humic-like (Peak A) and protein-like (Peak B) substance in SL were degraded (Gullian-Klanian et al., 2021; Zhou et al., 2023b).

Fluorescence parameters also supported the utilization of rDOM in SL. As shown in Fig. 3d, FI did not exhibit significant changes after treatment, because most of the rDOM in SL originated from the activated sludge in sewage treatment plant. However, the BIX increased, indicating that microbial activity in UASB-reactor generated SMP, which might be the peak C (Fig. 3c). The HIX decreased significantly, indicating a decrease in the humification of rDOM, which also validated the decrease in peak A (Fig. 3c, d).

To further investigate the utilization of rDOM in SL by this system, PARAFAC analysis was carried out based on EEM fluorescence spectroscopy data. Three components (C1-C3) of the rDOM in influent and effluent were identified by PARAFAC analysis (Table S2 and Fig. S2). As shown in Fig. 3e, the content of all three components has decreased after treatment, especially in C3. This supported the utilization of rDOM in SL was associated with the degradation of humic-like and protein-like compounds. Furthermore, the utilization of C3 was significantly higher than C1 and C2. Therefore, microorganisms mainly utilized protein-like substance as electron donor for nitrate reduction (Cao et al., 2019; Du et al., 2022).

### 3.2.3. FTICR-MS revealed the evolution of rDOM

FTICR-MS spectrometry was utilized to reveal the molecular

composition transformation of rDOM in SL after anammox treatment. There are seven groups of different molecular composition components based on elemental composition as shown in Fig. 4a-g. The rDOM composed with CHON, CHONP, CHONS, CHONPS and CHOS was extensively removed. In addition, the H/C was decreased in all components, indicating the degradation of rDOM in SL (Wu et al., 2023). Interestingly, the co-metabolism of carbon, nitrogen and sulfur also existed in this anammox reactor (Fig. 4a-d, f), which further proved protein-like component was significant utilized (Fig. 3e) and confirmed the efficient removal performance of the reactor for ON (Fig. 2).

Denitrifying bacteria utilized some of the rDOM in anammox reactor resulting in the decline in its molecular weight (Fig. 5a). Also, the relative intensity of each molecular weight decreased. Furthermore, the rDOM was also classified into seven groups according to H/C and O/C ratios (Fig. S3). This classification allowed for a more in-depth analysis of the transformation and utilization of the rDOM (Gu et al., 2023). In each group, rDOM contained CHO, CHON, CHOS and CHONS dominated (Fig. 5b, c). In addition, the relative abundance of all types of rDOM decreased from 46.81 % to 33.61 % except group III. Indicating lignins-like compounds were the most challenging to eliminate in this system, while protein-like compounds were the most easily utilized (Zhang et al., 2019). To provide additional insight into the molecular transformations post-treatment, the rDOM molecules were categorized into three groups: completely removed (detected solely in the influent, Fig. 5d), produced (detected solely in the effluent, Fig. 5e), and partially removed rDOM molecules (detected in both phases, yet with a lower relative abundance in the effluent compared to the influent, Fig. S4). The results suggested that the transformation preferably targeted rDOM featuring larger molecules along with unsaturated and aromatic groups. Meanwhile, the low abundance of group III in Fig. 5d while high abundance in Fig. 5e revealed that the rDOM was transformed to low H/C and low O/C substance, indicating denitrifying bacteria struggle to remove lignins-like compounds. Moreover, it underscores that lignin-like compounds have emerged as the predominant final destination for rDOM in SL.

To sum up, the efficient utilization of rDOM has significantly contributed to the advanced removal of nitrogen from SL in this reactor. Spectral data indicated that denitrifying bacteria may preferentially utilize protein-like compounds, followed by humic substances. Furthermore, post-treatment, rDOM in SL ultimately transformed into lignin-like compounds, and accumulated within the reactor.

## 3.3. Changes in microbial community structure

### 3.3.1. SEM revealed the changes in morphology

The morphological characteristics of sludge (including granular and

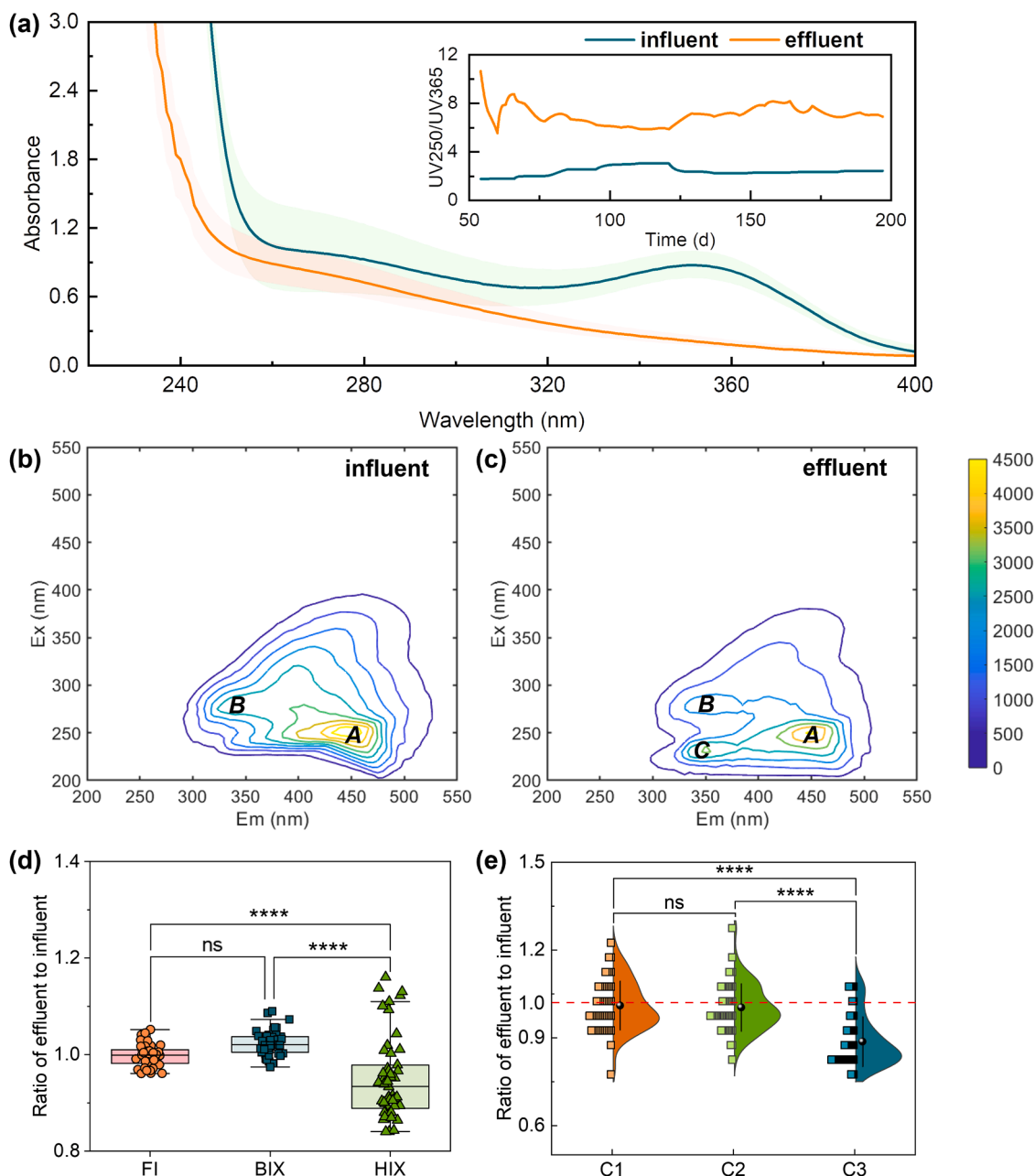


**Fig. 3.** (a) UV/Vis spectra of the sludge leachate treated by anammox reactor. Three-dimensional EEM spectra of rDOM in (b) influent and (c) effluent. Changes in (d) fluorescence parameters including fluorescence index (FI), biological index (BIX), humification index (HIX) and (e) three components in anammox reactor influent and effluent. (\*\*\*\*,  $p < 0.0001$ ; C1, microbial humic-like; C2, terrestrial humic-like; C3, protein-like).

floc sludge) collected in Stage I (day 1) and III (day 200) were investigated. Numerous spherical bacteria were identified within the granules (Fig. 6a, c), densely interconnected to create a network intertwined with EPS, hypothesized to be the anammox bacteria. However, short rod bacteria were distributed on the surface and inside floc sludge (Fig. 6b), along with visible EPS cohering the cells, which was assumed to be the denitrifying bacteria. In addition, filamentous bacteria were observed in granular sludge, which is benefit for sludge granular. These findings showed that the denitrifying bacteria proficient in the denitratation process may exhibited a preference for enrichment within flocs, while anammox bacteria may be more enriched in granular sludge (Du et al., 2023). Such spatial distribution of microorganisms facilitates better cooperation among them to achieve advanced nitrogen removal in treating SL.

### 3.3.2. Microbial sequencing specified the community succession

The total number of genera (with a relative abundance greater than 1 %) was 27, highlighting the microbial complexity and diversity (Fig. 6d). *Candidatus Brocadia* was the dominate anammox bacteria. Throughout the operation, the abundance of *Candidatus Brocadia* gradually decreased, ultimately stabilizing at approximately 2 %. However, the nitrogen removal performance of anammox was hardly affected, maintaining an exceptionally high removal rate of  $\text{NH}_4^+\text{-N}$  (Fig. 1a). Indicating an increase in the abundance of other functional bacterial communities and the successful coupling of functional communities within the synthetic platform.

Specifically, as shown in Fig. 6d, taxa belonging to the *Anaerolineaceae* genus such as *o\_SBR1031*, *OLB13*, *o\_RBG-13-54-9*, *f\_A4b*, *c\_OLB14* and *o\_Ardenticatenales* (Jiang et al., 2021, 2023). They had the ability to decompose rDOM (He et al., 2023; Jiang et al., 2021, 2023; Si et al.,

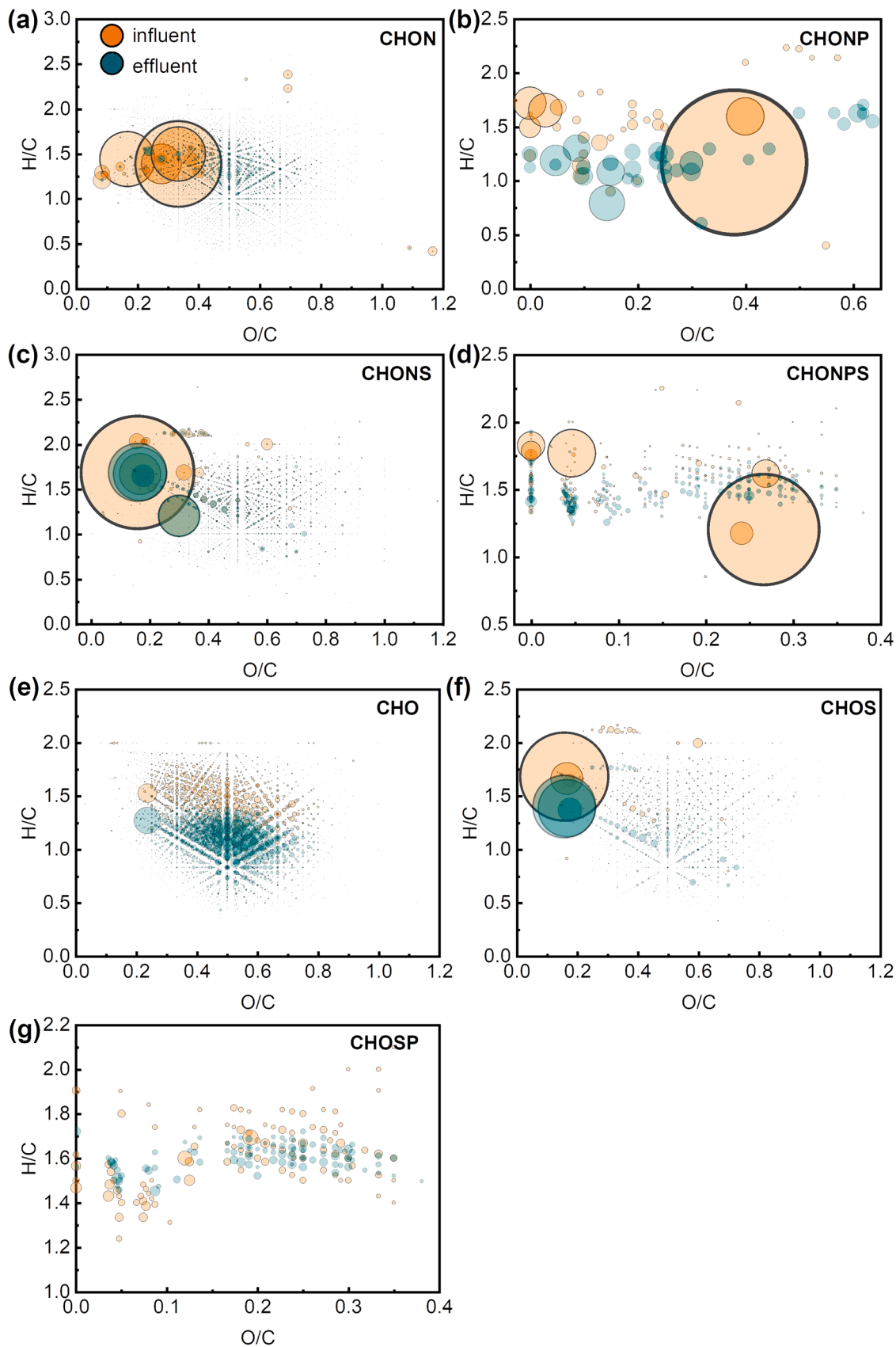
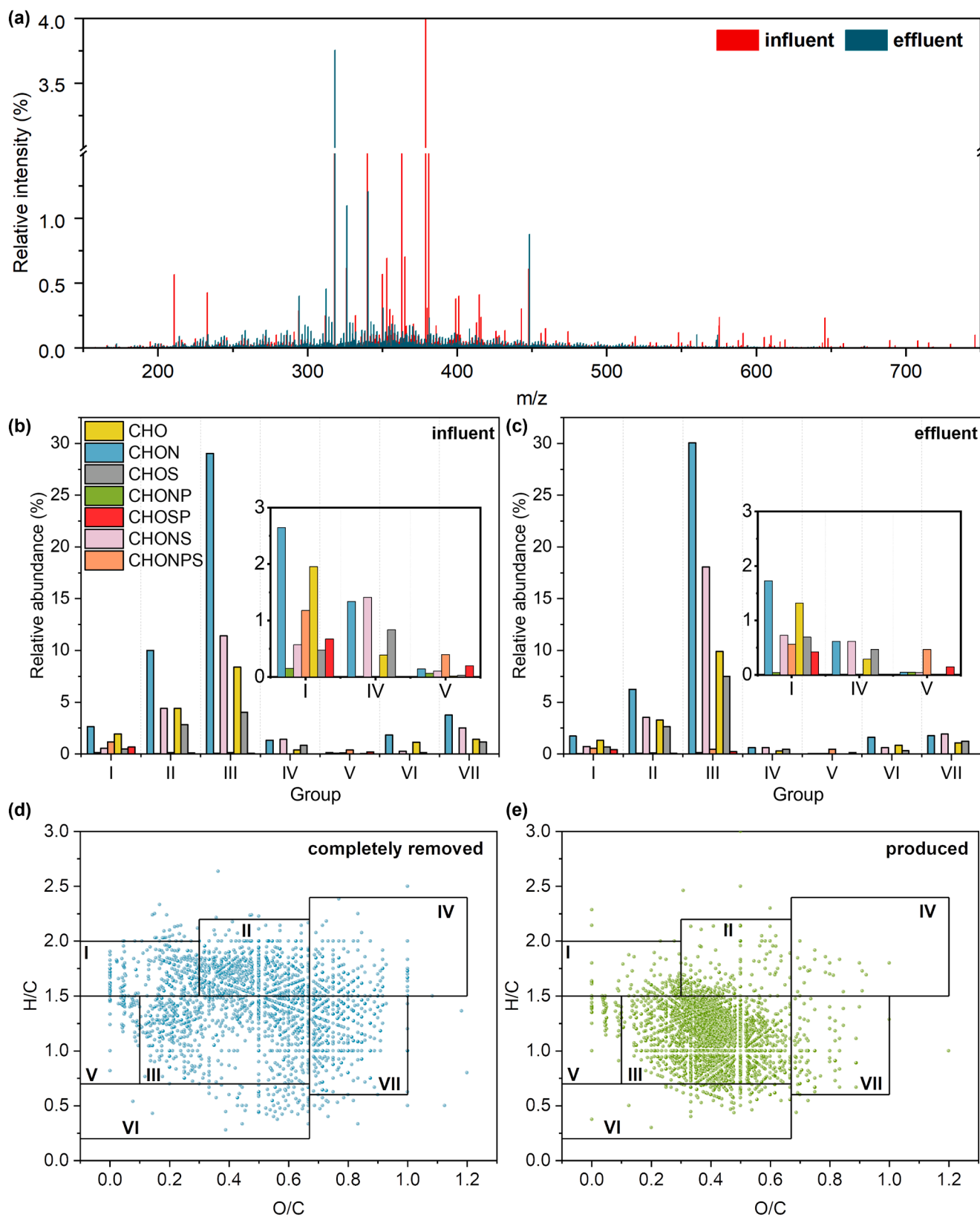


Fig. 4. VK diagrams describing the various rDOM formulas including (a) CHON, (b) CHONP, (c) CHONS, (d) CHONPS, (e) CHO, (f) CHOS and (g) CHOSP in influent and effluent. A larger dot size represented the higher relative intensity of the molecule in the rDOM.



**Fig. 5.** (a) Differences in molecular weight of rDOM in influent and effluent. Relative abundance of VK diagram-derived (Fig. S3) rDOM classification classes in influent (b), effluent (c). VK diagrams of the completely removed (d) and the produced (e) part rDOM. (I: lipids; II: proteins; III: lignins/carboxylic rich alicyclic molecules; IV: carbohydrates; V: unsaturated hydrocarbons; VI: condensed aromatic structures; and VII: tannins).



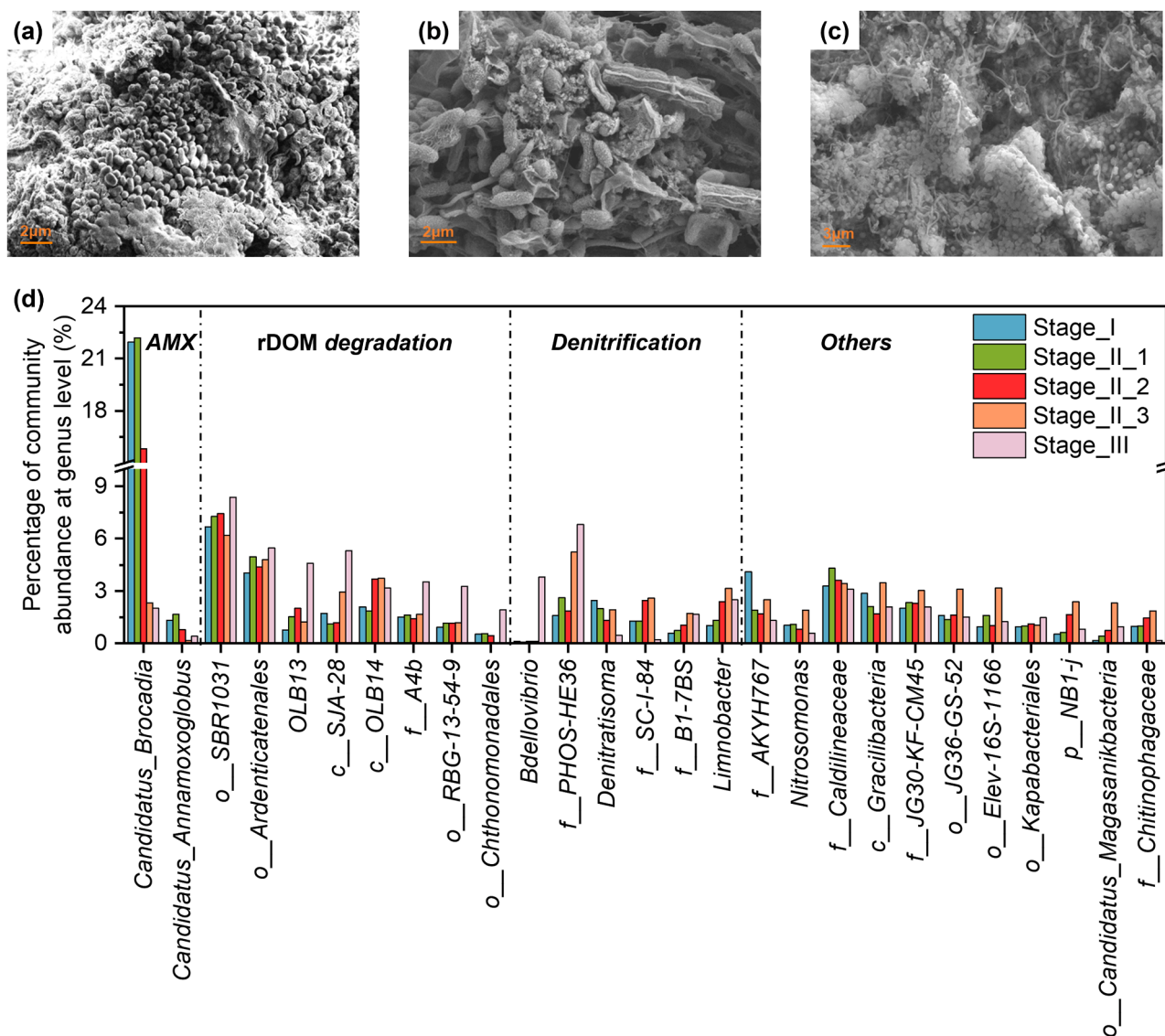


Fig. 6. SEM observation of sludge taken from anammox reactor on day 1 (a) and day 200 (b for floc sludge, c for granular sludge). (d) Relative abundance of the community structure component at genus level. Abbreviations: AMX, anammox.

2023; Zhao et al., 2023), their total relative abundance increased from 18.23 % to 35.62 %. Furthermore, the total relative abundance of genera associated with denitrification increased from 7.02 % to 15.44 %. Notably, the relative abundance of *Bdellovibrio* and *f*<sub>PHOS-HE36</sub> functional denitrification increased 8.91 % (Jiang et al., 2023; Qin et al., 2017; Zhao et al., 2023). These results indicated an enhanced capacity to utilize rDOM to provide electrons for nitrate reduction in this reactor.

### 3.4. Metabolisms of nitrogen and rDOM and their mechanisms

#### 3.4.1. Metabolisms of nitrogen

A comprehensive analysis of the functional genes and enzymes related to nitrogen metabolism was conducted to explore the potential interactions between denitrifying and anammox bacteria. In the process of SL treatment, the functional genes and related enzymes of anammox decreased, while most in denitrification process increased (Fig. 7). Meanwhile, the nitrogen removal performance in this system didn't decline but instead increased. This phenomenon indicated that under the influence of organic matter in SL, the nitrogen removal process shifted towards a combined action of both heterotrophic denitrification and anammox.

Interestingly, the *Nar* genes functional for the reduction of  $\text{NO}_3^-$ -N were approximately 7.6 times more abundant than those of *nirK* and *nirS* that responsible for the reduction of  $\text{NO}_2^-$ -N (Fig. 7a). Furthermore, within the array of highly abundant species engaged in the denitrification process, the expression level of *Nar* enzymes significantly surpassed that of *Nir* enzymes. In addition, the nitrate reductases encoded by *Nar* gain electrons directly from the quinone pool. However, the nitrite reductases (encoded by *nirS* or *nirK*) in the periplasmic space acquire electrons from the quinone pool through the transport relay from Complex III to soluble cytochrome c. The electrons used for denitrification initially come from the oxidation of NADH by complex I. Therefore, compared to Stage I, the substantial 54 % decrease in Complex III, coupled with a slight 7 % increase in Complex I (Fig. 7c), underscores the considerable potential of denitrification in supplying  $\text{NO}_2^-$ -N for anammox within this reactor (Zhang et al., 2022c). These results strongly demonstrated the occurrence of denitrification processes within this system (Du et al., 2024). This also explained why the anammox process could operate smoothly under extremely low influent RS conditions. Meanwhile, the *Nos* and *Nor* genes abundance increased (Fig. 7a), which indicated that the system in this study has the potential to significantly reduce  $\text{N}_2\text{O}$  and  $\text{NO}$  emissions.

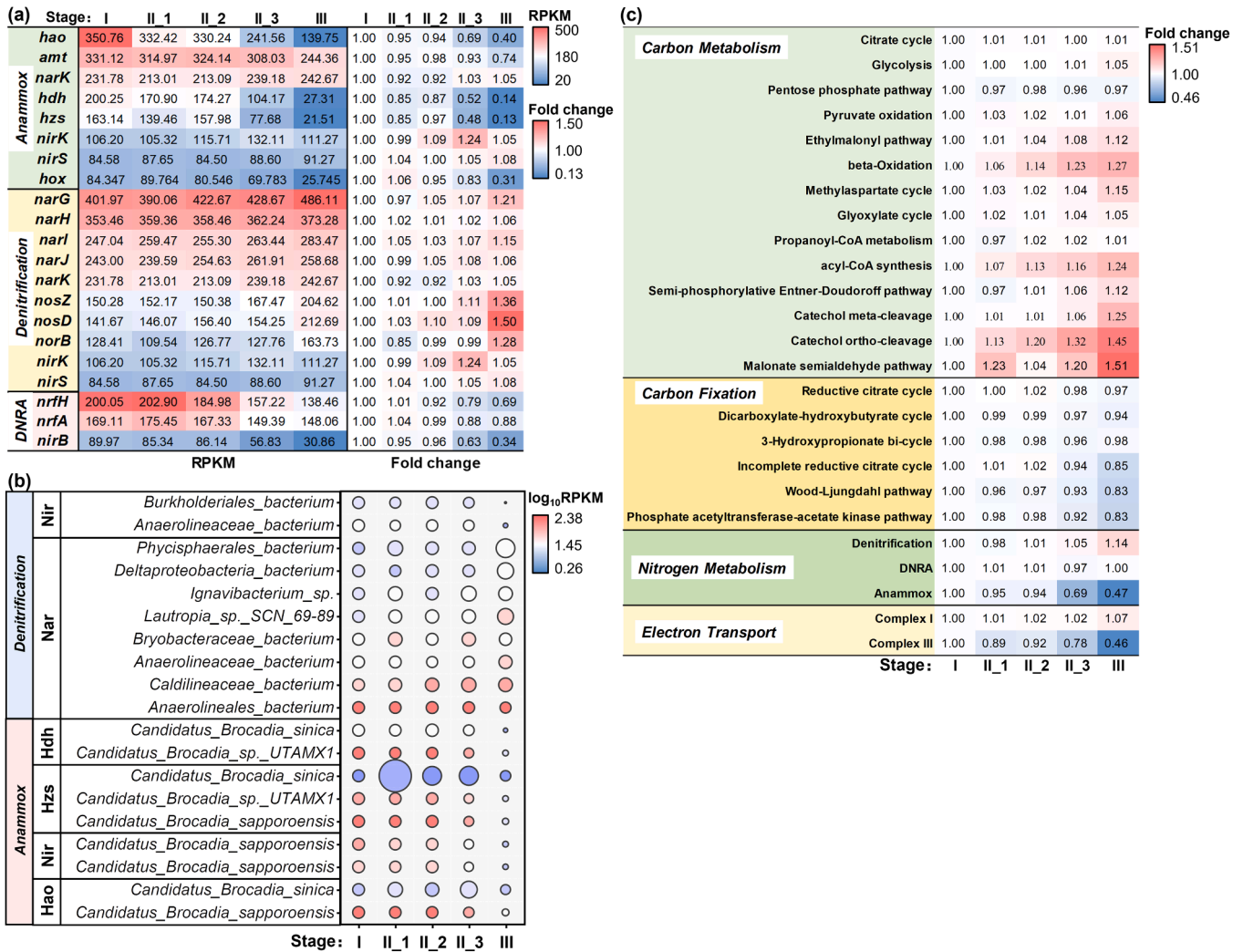


**Fig. 7.** Metagenomic analysis on nitrogen and carbon metabolism: (a) The abundance of nitrogen metabolic genes based on KEGG database. (b) Species and nitrogen removal contribution analysis based on COG database. (c) The changes of carbon, nitrogen metabolic, carbon fixation and electron transport modules based on KEGG database. (RPKM: Reads Per Kilobase Million; Fold change: Ratio between different stages and Stage I; The bubble size in the bubble chart (b) was determined by Fold change).

Moreover, *hzs*, *hao* and *hdh*, accordingly encoding hydrazine synthase and hydrazine dehydrogenase responsible for the anammox process, exhibited a significantly decreasing abundance from 163.14, 350.76 and 200.25 to 21.25, 139.75 and 27.31, accounting for approximately 86.81 %, 86.36 %, and 60.16 % of their initial levels (Fig. 7a). However, the related enzymes didn't exhibit a sharp reduction, showing approximately 25.49 % for Hao enzymes, 32.66 % for Hzs enzymes and 51.14 % for Hdh enzymes (Fig. 7b). These results further suggested the favorable nitrogen removal efficiency.

Notably, the dissimilatory nitrate reduction to ammonium (DNRA) pathway coupled with anammox process could also lead to a similar nitrogen removal efficiency (Ahmad et al., 2021; Wang et al., 2022b; Zhou et al., 2023a). However, as shown in Fig. 7a, the abundances of DNRA related genes, *nrFA*, *nrFH* and *nirB* gradually decreased. In addition, the DNRA module has not been strengthened in this reactor either (Fig. 7c), indicating that nitrate removal is not dominated by DNRA process.

To sum up, metagenomic analysis in nitrogen metabolism suggested the concurrent presence of denitrification and anammox process and their synergy. In addition, the nitrate reduction was dominated by denitrification rather than DNRA process.

#### 3.4.2. Metabolisms of rDOM

The rDOM in SL played a significant role in the advanced nitrogen removal process. Interestingly, the carbon metabolism-related modules all exhibited an increase, while the carbon fixation-related modules decreased, mirroring the trends observed in the denitrification and anammox modules (Fig. 7c). This indicated an enhanced utilization of rDOM in SL by denitrification process, while the abundance of anammox declined, the findings presented here align with the microbial sequencing results (Fig. 6d). Briefly, during rDOM metabolism, the refractory organics in SL were first hydrolyzed by the hydrolysis bacteria and then produced acetate by the acidogenesis bacteria (Ji et al., 2020). Finally, the organic matters in SL entered the tricarboxylic acid cycle (TCA), generating NADH that transferred electrons to complex I, providing electrons for nitrate reduction.

#### 3.4.3. Proposed mechanism

To sum up, in the process of treating SL using anammox process, the rDOM in SL triggered the coupling of denitrification and anammox. As shown in Fig. 8, the bulk  $\text{NO}_2^-$ -N and bulk  $\text{NH}_4^+$ -N were removed in the anammoxosome accompanied by the production of  $\text{NO}_3^-$ -N. Without the coupling of denitrification, the theoretical maximum TIN removal efficiency of this system is 89 % owing to the production of  $\text{NO}_3^-$ -N (Jiang et al., 2023). Simultaneously, the rDOM in SL was utilized by

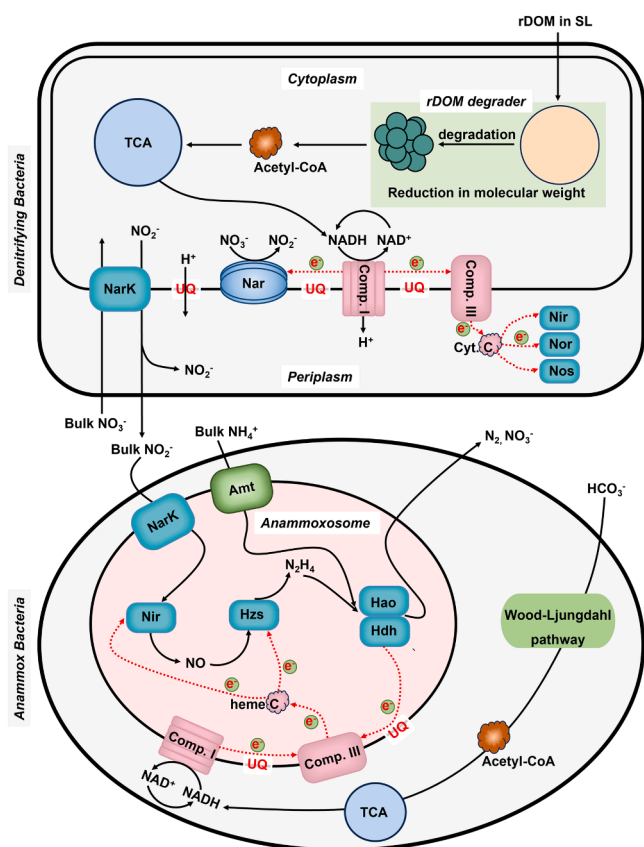


Fig. 8. Mechanism of cooperation between denitrification and anammox in treating SL.

heterotrophic bacteria belonging to the *Anaerolineaceae* genus functioned with rDOM degradation, where large organic molecules are broken down into smaller ones. Then, denitrification bacteria reducing nitrate to nitrite that served as a substrate for the anammox process. Notably, thanks to the existence of heterotrophic and denitrifying bacteria, most ON was also removed. Both denitrification activity and anammox activity could be mutually promoted for advanced nitrogen removal performance in treating SL.

#### 4. Conclusion

This study demonstrated the feasibility and high efficiency of using rDOM triggered denitrification-anammox for treating sludge leachate. In this reactor, a high nitrogen removal rate for SL was achieved, with  $4.27 \pm 0.45$  mgTN/L and  $5.58 \pm 1.64$  mgTN/L in effluent during the stable treatment period. During the long-term operation, spectral evidences of rDOM in SL indicated their utilization by denitrifying bacteria. The protein-like compounds were utilized firstly to supply nitrite for anammox process, while struggle to lignins, leading to an approximately  $65.17\% \pm 1.71\%$  COD removal rate. Meanwhile, there was a notable increase in the relative abundance of genera involved in rDOM utilization, rising from 18.23% to 35.62%. The metagenomic data revealed the combination of denitrification and anammox, where anammox bacteria were predominantly found in granular sludge, whereas denitrifying bacteria were more prevalent in floc sludge. Notably, *Candidatus Brocadia* had the highest abundance in anammox bacteria for nitrogen removal. Overall, this study presented a synergy platform for advanced nitrogen removal utilizing *in-situ* rDOM in low C/N ratio wastewater (without the need for additional carbon sources).

#### CRediT authorship contribution statement

**Ben Dai:** Writing – review & editing, Writing – original draft, Methodology, Data curation, Conceptualization. **Yifeng Yang:** Project administration, Funding acquisition. **Zuobin Wang:** Writing – review & editing. **Jingzhou Zhou:** Writing – review & editing, Visualization. **Zhenyu Wang:** Writing – review & editing. **Xin Zhang:** Writing – review & editing. **Siqing Xia:** Project administration, Funding acquisition.

#### Declaration of competing interest

The authors declare no competing interests.

#### Data availability

Data will be made available on request.

#### Acknowledgements

This work was supported by National Key Project of Research and Development Plan of China (2021YFC3201300) and Shanghai Sailing Program (21YF1443900).

#### Supplementary materials

Supplementary material associated with this article can be found, in the online version, at [doi:10.1016/j.watres.2024.121678](https://doi.org/10.1016/j.watres.2024.121678).

#### References

- Ahmad, H.A., Guo, B., Zhuang, X., Zhao, Y., Ahmad, S., Lee, T., Zhu, J., Dong, Y., Ni, S.-Q., 2021. A twilight for the complete nitrogen removal via synergistic partial-denitrification, anammox, and DNRA process. *npj Clean Water* 4, 1–11. <https://doi.org/10.1038/s41545-021-00122-5>.
- Apha, 1985. *Standard Methods For the Examination of Water and Wastewater*. Apha.
- Cao, S., Sun, F., Lu, D., Zhou, Y., 2019. Characterization of the refractory dissolved organic matters (rDOM) in sludge alkaline fermentation liquid driven denitrification: effect of HRT on their fate and transformation. *Water Res.* 159, 135–144. <https://doi.org/10.1016/j.watres.2019.04.063>.
- Chen, H., Ye, Q., Wang, X., Sheng, J., Yu, X., Zhao, S., Zou, X., Zhang, W., Xue, G., 2024. Applying sludge hydrolysate as a carbon source for biological denitrification after composition optimization via red soil filtration. *Water Res.* 249, 120909 <https://doi.org/10.1016/j.watres.2023.120909>.
- Chen, W., Gu, Z., Wen, P., Li, Q., 2019. Degradation of refractory organic contaminants in membrane concentrates from landfill leachate by a combined coagulation-ozonation process. *Chemosphere* 217, 411–422. <https://doi.org/10.1016/j.chemosphere.2018.11.002>.
- Chen, W., He, C., Gu, Z., Wang, F., Li, Q., 2020. Molecular-level insights into the transformation mechanism for refractory organics in landfill leachate when using a combined semi-aerobic aged refuse biofilter and chemical oxidation process. *Sci. Total Environ.* 741, 140502 <https://doi.org/10.1016/j.scitotenv.2020.140502>.
- Dai, B., Yang, Y., Wang, Zuobing, Wang, J., Yang, L., Cai, X., Wang, Zhenyu, Xia, S., 2023. Enhancement and mechanisms of iron-assisted anammox process. *Sci. Total Environ.* 858, 159931 <https://doi.org/10.1016/j.scitotenv.2022.159931>.
- de Graaff, M.S., Temmink, H., Zeeman, G., van Loosdrecht, M.C.M., Buisman, C.J.N., 2011. Autotrophic nitrogen removal from black water: calcium addition as a requirement for settleability. *Water Res.* 45, 63–74. <https://doi.org/10.1016/j.watres.2010.08.010>.
- Du, R., Liu, Q., Li, C., Li, X., Cao, S., Peng, Y., 2023. Spatiotemporal assembly and immigration of heterotrophic and anammox bacteria allow a robust synergy for high-rate nitrogen removal. *Environ. Sci. Technol.* 57, 9075–9085. <https://doi.org/10.1021/acs.est.2c08034>.
- Du, R., Liu, Q., Xu, X., Horn, H., Cao, S., Peng, Y., 2024. Enhancing competitiveness of anammox bacteria with domestic wastewater as electron donor for nitrate-preferential denitrification: experimental evidence and metagenomic mechanism. *ACS Sustain. Chem. Eng.* <https://doi.org/10.1021/acssuschemeng.3c06523>.
- Du, R., Peng, Y., Cao, S., 2022. Insights into size-fractionated anammox granules presented with refractory organics from municipal wastewater-driven partial denitrification to improve the synergy of anammox and denitrification. *J. Clean. Prod.* 378, 134526 <https://doi.org/10.1016/j.jclepro.2022.134526>.
- Du, R., Peng, Y., Cao, S., Wang, S., Wu, C., 2015. Advanced nitrogen removal from wastewater by combining anammox with partial denitrification. *Bioresour. Technol.* 179, 497–504. <https://doi.org/10.1016/j.biortech.2014.12.043>.
- Du, R., Peng, Y., Ji, J., Shi, L., Gao, R., Li, X., 2019. Partial denitrification providing nitrite: opportunities of extending application for anammox. *Environ. Int.* 131, 105001 <https://doi.org/10.1016/j.envint.2019.105001>.

- Gu, Z., Bao, M., He, C., Chen, W., 2023. Transformation of dissolved organic matter in landfill leachate during a membrane bioreactor treatment. *Sci. Total Environ.* 856, 159066 <https://doi.org/10.1016/j.scitotenv.2022.159066>.
- Gullian-Klanian, M., Gold-Bouchot, G., Delgadillo-Dfiaz, M., Aranda, J., Sánchez-Solis, M. J., 2021. Effect of the use of *Bacillus* spp. on the characteristics of dissolved fluorescent organic matter and the phytochemical quality of *Stevia rebaudiana* grown in a recirculating aquaponic system. *Environ. Sci. Pollut. Res.* 28, 36326–36343. <https://doi.org/10.1007/s11356-021-13148-6>.
- He, W., Zhong, Q., Liu, J., Cai, J., Luo, X., Yuan, Y., 2023. Microbially mediated molecular transformations of dissolved organic matter in bioelectrochemical systems treating beer brewery wastewater. *Chem. Eng. J.* 461, 142111 <https://doi.org/10.1016/j.cej.2023.142111>.
- He, X.-S., Xi, B.-D., Zhang, Z.-Y., Gao, R.-T., Tan, W.-B., Cui, D.-Y., Yuan, Y., 2015. Composition, removal, redox, and metal complexation properties of dissolved organic nitrogen in composting leachates. *J. Hazard. Mater.* 283, 227–233. <https://doi.org/10.1016/j.jhazmat.2014.09.027>.
- Hou, X., Li, X., Zhu, X., Li, W., Kao, C., Peng, Y., 2024. Advanced nitrogen removal from municipal wastewater through partial nitrification-denitrification coupled with anammox in step-feed continuous system. *Bioresour. Technol.* 391, 129967 <https://doi.org/10.1016/j.biortech.2023.129967>.
- Ji, J., Peng, Y., Wang, B., Li, X., Zhang, Q., 2020. Synergistic Partial-Denitrification, Anammox, and in-situ Fermentation (SPDAF) process for advanced nitrogen removal from domestic and nitrate-containing wastewater. *Environ. Sci. Technol.* 54, 3702–3713. <https://doi.org/10.1021/acs.est.9b07928>.
- Jia, F., Yang, Q., Liu, X., Li, X., Li, B., Zhang, L., Peng, Y., 2017. Stratification of Extracellular Polymeric Substances (EPS) for aggregated anammox microorganisms. *Environ. Sci. Technol.* 51, 3260–3268. <https://doi.org/10.1021/acs.est.6b05761>.
- Jiang, C., Tang, X., Peng, F., Zhao, J., Liu, Z., Qu, C., Adhikary, K.K., Wu, D., Tang, C.-J., 2022. Distinct membrane fouling characteristics of anammox MBR with low  $\text{NO}_2^-/\text{NH}_4^+$ -N ratio. *Sci. Total Environ.* 817, 152994 <https://doi.org/10.1016/j.scitotenv.2022.152994>.
- Jiang, H., Wang, Z., Ren, S., Qiu, J., Li, X., Peng, Y., 2021. Culturing sludge fermentation liquid-driven partial denitrification in two-stage Anammox process to realize advanced nitrogen removal from mature landfill leachate. *J. Hazard. Mater.* 415, 125568 <https://doi.org/10.1016/j.jhazmat.2021.125568>.
- Jiang, M., Ji, S., Wu, R., Yang, H., Li, Y.-Y., Liu, J., 2023. Exploiting refractory organic matter for advanced nitrogen removal from mature landfill leachate via anammox in an expanded granular sludge bed reactor. *Bioresour. Technol.* 371, 128594 <https://doi.org/10.1016/j.biortech.2023.128594>.
- Kartal, B., Kuenen, J.G., van Loosdrecht, M.C.M., 2010. Sewage treatment with anammox. *Science* 328, 702–703. <https://doi.org/10.1126/science.1185941>.
- Li, Z., Kecheh, X., Yongzhen, P., 2018. Composition characterization and transformation mechanism of refractory dissolved organic matter from an ANAMMOX reactor fed with mature landfill leachate. *Bioresour. Technol.* 250, 413–421. <https://doi.org/10.1016/j.biortech.2017.11.007>.
- Liu, S., Cai, C., Sun, F., Ma, M., An, T., Chen, C., 2024. Advanced nitrogen removal of landfill leachate treatment with anammox process: a critical review. *J. Water Process Eng.* 58, 104756 <https://doi.org/10.1016/j.jwpe.2023.104756>.
- Lu, Y.-Z., Li, N., Ding, Z.-W., Fu, L., Bai, Y.-N., Sheng, G.-P., Zeng, R.J., 2017. Tracking the activity of the Anammox-DAMO process using excitation-emission matrix (EEM) fluorescence spectroscopy. *Water Res.* 122, 624–632. <https://doi.org/10.1016/j.watres.2017.06.036>.
- Osburn, C.L., Handsel, L.T., Peierls, B.L., Paerl, H.W., 2016. Predicting sources of dissolved organic nitrogen to an estuary from an agro-urban coastal watershed. *Environ. Sci. Technol.* 50, 8473–8484. <https://doi.org/10.1021/acs.est.6b00053>.
- Qin, Y., Cao, Y., Ren, J., Wang, T., Han, B., 2017. Effect of glucose on nitrogen removal and microbial community in anammox-denitrification system. *Bioresour. Technol.* 244, 33–39. <https://doi.org/10.1016/j.biortech.2017.07.124>.
- Renou, S., Givaudan, J.G., Poulain, S., Dirassouyan, F., Moulin, P., 2008. Landfill leachate treatment: review and opportunity. *J. Hazard. Mater.* 150, 468–493. <https://doi.org/10.1016/j.jhazmat.2007.09.077>.
- Si, C., Wang, S., Chen, Z., Hu, G., Zhao, X., Sun, P., Zhang, Q., Jiang, W., 2023. Enhanced denitrification using high-molecular-weight poly(lactic acid) blended with lactide as an effective carbon source. *Bioresour. Technol.* 387, 129542 <https://doi.org/10.1016/j.biortech.2023.129542>.
- Song, X., Kong, F., Liu, B.-F., Song, Q., Ren, N.-Q., Ren, H.-Y., 2024. Combined transcriptomic and metabolomic analyses of temperature response of microalgae using waste activated sludge extracts for promising biodiesel production. *Water Res.* 251, 121120 <https://doi.org/10.1016/j.watres.2024.121120>.
- Wang, H., Fan, Y., Zhou, M., Wang, W., Li, X., Wang, Y., 2022a. Function of Fe(III)-minerals in the enhancement of anammox performance exploiting integrated network and metagenomics analyses. *Water Res.* 210, 117998 <https://doi.org/10.1016/j.watres.2021.117998>.
- Wang, W., Wang, T., Liu, Q., Wang, H., Xue, H., Zhang, Z., Wang, Y., 2022b. Biochar-mediated DNRA pathway of anammox bacteria under varying COD/N ratios. *Water Res.* 212, 118100 <https://doi.org/10.1016/j.watres.2022.118100>.
- Wang, Y., Lin, Z., He, L., Huang, W., Zhou, J., He, Q., 2019. Simultaneous partial nitrification, anammox and denitrification (SNAD) process for nitrogen and refractory organic compounds removal from mature landfill leachate: performance and metagenome-based microbial ecology. *Bioresour. Technol.* 294, 122166 <https://doi.org/10.1016/j.biortech.2019.122166>.
- Wu, B., Ran, T., Liu, S., Li, Q., Cui, X., Zhou, Y., 2023. Biofilm bioactivity affects nitrogen metabolism in a push-flow microalgae-bacteria biofilm reactor during aeration-free greywater treatment. *Water Res.* 244, 120461 <https://doi.org/10.1016/j.watres.2023.120461>.
- Wu, L., Li, Z., Zhao, C., Liang, D., Peng, Y., 2018. A novel partial-denitrification strategy for post-anammox to effectively remove nitrogen from landfill leachate. *Sci. Total Environ.* 633, 745–751. <https://doi.org/10.1016/j.scitotenv.2018.03.213>.
- Wu, R., Li, Y.-Y., Liu, J., 2022. Refractory dissolved organic matter as carbon source for advanced nitrogen removal from mature landfill leachate: a review and prospective application. *J. Clean. Prod.* 380, 134962 <https://doi.org/10.1016/j.jclepro.2022.134962>.
- Xiao, R., Ni, B.-J., Liu, S., Lu, H., 2021. Impacts of organics on the microbial ecology of wastewater anammox processes: recent advances and meta-analysis. *Water Res.* 191, 116817 <https://doi.org/10.1016/j.watres.2021.116817>.
- Xie, C., Zhang, Q., Li, X., Dan, Q., Qin, L., Wang, C., Wang, S., Peng, Y., 2023. Highly efficient transformation of slowly-biodegradable organic matter into endogenous polymers during hydrolytic fermentation for achieving effective nitrite production by endogenous partial denitrification. *Water Res.* 230, 119537 <https://doi.org/10.1016/j.watres.2022.119537>.
- Xiong, L., Li, X., Li, J., Zhang, Q., Zhang, L., Wu, Y., Peng, Y., 2023. Efficient nitrogen removal from real municipal wastewater and mature landfill leachate using partial nitrification-simultaneous anammox and partial denitrification process. *Water Res.* 121088 <https://doi.org/10.1016/j.watres.2023.121088>.
- Xu, Y., Wu, Y., Zhang, X., Chen, G., 2021. Effects of freeze-thaw and chemical preconditioning on the consolidation properties and microstructure of landfill sludge. *Water Res.* 200, 117249 <https://doi.org/10.1016/j.watres.2021.117249>.
- Yin, R., Zhou, S., Lu, D., Diao, S., Shi, W., Gong, H., Dai, X., 2023. Evolution of dissolved organic nitrogen (DON) during sludge reject water treatment revealed by FTICR-MS. *Sci. Total Environ.* 893, 164944 <https://doi.org/10.1016/j.scitotenv.2023.164944>.
- Zhang, D., Peng, Y., Huang, H., Khunjar, W., Wang, Z.-W., 2020. Recalcitrant dissolved organic nitrogen formation in thermal hydrolysis pretreatment of municipal sludge. *Environ. Int.* 138, 105629 <https://doi.org/10.1016/j.envint.2020.105629>.
- Zhang, F., Peng, Y., Liu, Y., Zhao, L., 2021. Improving stability of mainstream Anammox in an innovative two-stage process for advanced nitrogen removal from mature landfill leachate. *Bioresour. Technol.* 340, 125617 <https://doi.org/10.1016/j.biortech.2021.125617>.
- Zhang, F., Peng, Y., Wang, Z., Jiang, H., Ren, S., Qiu, J., Zhang, L., 2022a. An innovative process for mature landfill leachate and waste activated sludge simultaneous treatment based on Partial Nitrification, in situ Fermentation, and Anammox (PNFA). *Environ. Sci. Technol.* 56, 1310–1320. <https://doi.org/10.1021/acs.est.1c06049>.
- Zhang, J., Peng, Y., Li, X., Du, R., 2022b. Feasibility of partial-denitrification/anammox for pharmaceutical wastewater treatment in a hybrid biofilm reactor. *Water Res.* 208, 117856 <https://doi.org/10.1016/j.watres.2021.117856>.
- Zhang, L., Peng, Y., Ge, Z., Xu, K., 2019. Fate of dissolved organic nitrogen during the Anammox process using ultra-high resolution mass spectrometry. *Environ. Int.* 131, 105042 <https://doi.org/10.1016/j.envint.2019.105042>.
- Zhang, Z., Zhang, Y., Shi, Z., Chen, Y., 2022c. Linking genome-centric metagenomics to kinetic analysis reveals the regulation mechanism of hydroxylamine in nitrite accumulation of biological denitrification. *Environ. Sci. Technol.* 56, 10317–10328. <https://doi.org/10.1021/acs.est.2c01914>.
- Zhao, Y., Li, J., Liu, Q., Qi, Z., Li, X., Zhang, Q., Sui, J., Wang, C., Peng, Y., 2023. Fast start-up and stable operation of mainstream anammox without inoculation in an A2/O process treating low COD/N real municipal wastewater. *Water Res.* 231, 119598 <https://doi.org/10.1016/j.watres.2023.119598>.
- Zhou, J., Wu, C., Pang, S., Yang, L., Yao, M., Li, X., Xia, S., Rittmann, B.E., 2022. Dissimilatory and cytoplasmic antimonate reductions in a hydrogen-based membrane biofilm reactor. *Environ. Sci. Technol.* 56, 14808–14816. <https://doi.org/10.1021/acs.est.2c04939>.
- Zhou, L., Zhao, B., Zhuang, W.-Q., 2023a. Double-edged sword effects of dissimilatory nitrate reduction to ammonium (DNRA) bacteria on anammox bacteria performance in an MBR reactor. *Water Res.* 233, 119754 <https://doi.org/10.1016/j.watres.2023.119754>.
- Zhou, X., Johnston, S.E., Bogard, M.J., 2023b. Organic matter cycling in a model restored wetland receiving complex effluent. *Biogeochemistry* 162, 237–255. <https://doi.org/10.1007/s10533-022-01002-x>.